VA RESEARCH & DEVELOPMENT

JRRD
Journal of Rehabilitation Research & Development
Vol. 36 No. 3, July 1999

Knee kinetics during functional electrical stimulation induced cycling in subjects with spinal cord injury: A preliminary study

John C. Franco, MD, MS; Karen L. Perell, PhD; Robert J. Gregor, PhD; A.M. Erika Scremin, MD

Department of Orthopedics, University of New Mexico, Albuquerque, NM; Physical Medicine & Rehabilitation Department, VA Greater Los Angeles Healthcare System--West Los Angeles Healthcare Center, Los Angeles, CA; Department of Medicine, Division of Physical Medicine and Rehabilitation, University of California Los Angeles, Los Angeles, CA; Department of Physical Therapy, Mount St. Mary's College, Los Angeles, CA; Department of Health and Performance Sciences, Georgia Institute of Technology, Atlanta, GA

Abstract--The purpose of this preliminary study was to describe pedal effectiveness parameters and knee-joint reaction forces generated by subjects with chronic spinal cord injury (SCI) during functional electrical stimulation (FES)-induced bicycling. Three male subjects (age 33--36 years old), who were post-traumatic SCI (ASIA-modified level A, level T4-C5) and enrolled in an FES rehabilitation program, signed informed consent forms and participated in this study. Kinematic data and pedal forces during bicycling were collected and effective force, knee-joint reaction forces, knee generalized muscle moments, and knee-joint power and work were calculated. There were three critical findings of this study: 1) pedaling effectiveness was severely compromised in this subject population as indicated by a lack of overall positive crank work; 2) knee-joint kinetics were similar in magnitude to data reported for unimpaired individuals pedaling at higher rates and workloads, suggesting excessive knee-joint loading for subjects with SCI; and 3) shear reaction forces and muscle moments were opposite in direction to data reported for unimpaired individuals, revealing an energetically unfavorable knee stabilizing mechanism. The critical findings of this study suggest that knee-joint kinetics may be large enough to produce a fracture in the compromised lower limbs of individuals with SCI.

Key words: *bicycling, biomechanics, joint reaction forces, kinetics, knee joint, osteopenia, spinal cord injured.*

INTRODUCTION

It is estimated that there are currently 500,000 people with spinal cord injuries (SCI) in the United States, with an annual incidence of 10,000 (1). However, while dramatic improvements in care have extended the average life span of individuals with SCI, disuse osteoporosis and the resulting complications remain a significant problem. These complications include immobilization hypercalcemia and fractures and are due primarily to decreased bone density (2).

It has long been understood that bone, like muscle and tendon, responds to load. Lack of compression forces on bone during bed rest, immobilization, and space flight, for example, causes bone mineral loss (3-5), decreased cortical bone density (6), abnormal osteoblastic/osteoclastic rates (7), loss of calcium (4,5,7), and changes in the mechanical properties (8,9). Intermittent loading as experienced during exercise, however, may have a sparing effect on bone loss. For example, when preventive exercise programs were initiated during space flight, a reduction in bone loss was observed (4,5). Animals subjected to artificial gravity during space flight had less bone loss, more rapid recovery of bone density upon return, and prevention of decreased femoral breaking strength (4).

While loss of tissue integrity is an important problem in persons with spinal cord injury, understanding the possible ameliorating effects of exercise is also important. Acute changes in environmental loads may cause tissue failure, while repetitive loading in certain exercise regimens will modify bone, muscle, tendon, and ligaments to respond more strongly to changes in environmental

loads. Exercises then must be prescribed such that they employ loading patterns designed to strengthen the compromised tissues in persons with spinal cord injury, while not exceeding possible failure thresholds.

Interventions such as functional electrical stimulation (FES) exercises and standing postural therapy do not appear to increase bone density in subjects with chronic, greater than 12-months, postinjury (1,10-14). While FES-induced cycling is a popular modality, the effect of the intermittent loads experienced during this task have not been quantified. Hence, their effect on bone and joints, for example, remains unknown. Intermittent loads transmitted through the knee joint during upright bicycling in unimpaired individuals are typically represented by axial (compressive/tensile) and shear (anteriorly/posteriorly directed) joint reaction force components. Axial components are compressive during the entire cycle with peak force (-250 N) at approximately 90° of the pedal cycle. Subsequent to this peak value, a rapid decrease in the compressive force component occurs at the end of the power phase and can remain under -50 N during the remainder of the pedal cycle. The shear components, on the other hand, are anteriorly directed during the power phase (0-180°) with peak force (120 N) at approximately 90° of the pedal cycle and slightly posteriorly directed during the recovery phase--180-360° (15).

Measures of pedal effectiveness such as effective force (force responsible for turning the crank in the appropriate direction) and mechanical power and work reflect performance efficiency (16,17). While these parameters have been studied extensively in elite bicyclists (17) and selected clinical population - cerebrovascular accidents (CVAs), for example (18), these parameters have not been studied during FES-induced bicycling in the SCI population. These parameters may provide insight into any limitations FES systems have in transmitting power to the bicycle to maintain pedaling rate. In response to the dearth of information on the kinetics of FES-induced cycling, we have constructed a set of novel strain gauge bicycle pedals capable of measuring normal and tangential pedal forces to understand the mechanical loading and efficiency during FES-induced exercise on the bicycle. The purpose of this preliminary study was to describe the knee-joint reaction forces and pedal effectiveness parameters generated by subjects with chronic SCI during FES-induced bicycling.

METHODS

Subjects

Three male subjects, all post-traumatic SCI (ASIA-modified level A, Ashworth spasticity 2-4) and enrolled in an FES rehabilitation program, signed informed consent forms approved by the VA Greater Los Angeles Healthcare System IRB and Research Committees, and participated in this study (**Table 1**). Subjects had received, previous to this investigation, varying degrees of FES rehabilitation--protocol and set-up were described in BeDell et al. (1). Subject A had just started FES rehabilitation without any practice on the bicycle; Subject B participated in a 3-week quadriceps strengthening FES program with minimal practice on the bicycle; and Subject C was nearing the completion of a one-year FES bicycling intervention. Each subject received a complete history and physical examination, reporting no history of parathyroid or thyroid disease. Each subject had baseline laboratory tests (calcium, phosphate, alkaline phosphates, sodium potassium, chloride, hemoglobin, and hematocrit), routine urinalysis, urine culture and sensitivity, resting electrocardiogram, and radiographs to rule out any other etiology that could contribute to osteoporosis. Radiographic studies included anterior/posterior and lateral lumbosacral spine films, pelvic, femoral, tibial, and feet films.

Table 1.

Demographic and anthropometric data for each subject.

Subject	Post-injury	Level	Age	Weight	Height
A	11	T9	36	65.25	175.30
B	11	T4	33	72.00	180.30
C	11	C5	33	60.75	186.70

Subj. = subject; Postinjury in years; Level = injury level; Age in years; Weight in kg; Height in cm.

Experimental Set-up

All data were collected on a REGYS1 ergometer (Therapeutic Alliance, Fairborn, OH). A detailed description of this apparatus and its operation have been published by Ragnarsson et al. (19). To summarize, the ergometry system consists of a microprocessor, a cycle ergometer, and an adjustable chair. The rider was secured to the chair by a chest harness and waist strap. Each thigh was attached to a stabilizing bar that minimized all thigh movement outside the sagittal plane. Each foot was inserted into a plastic boot designed to minimize ankle movement. Carbon-filled silastic surface electrodes (Therapeutic Alliance) were placed over the quadriceps, hamstring, and gluteal muscle groups, bilaterally. Stimulation parameters were as follows: intensity = 10-132 mA; pulse

frequency = 30 Hz; pulse duration = 400 µsec[1]. A set of sensors provided feedback on leg position to the bicycle control unit. A 2-minute warm-up phase was facilitated by an assistant while the stimulation was typically at 50 percent threshold values set prior to the beginning of bicycling. After the 2-minute warm-up period, muscle contraction was induced completely by the microprocessor, which sensed crank position to coordinate the phases of muscle stimulation. The stimulation paradigm utilized by the microprocessor is illustrated in **Figure 1.** As each subject proceeded with the bicycling task, stimulus intensity was modulated to maintain a target crank velocity of 50 revolutions per minute (RPM). When the crank velocity fell below 35 RPM at maximum stimulus intensity (132 mA), the microprocessor ended the exercise session and a 2-minute cool-down phase began.

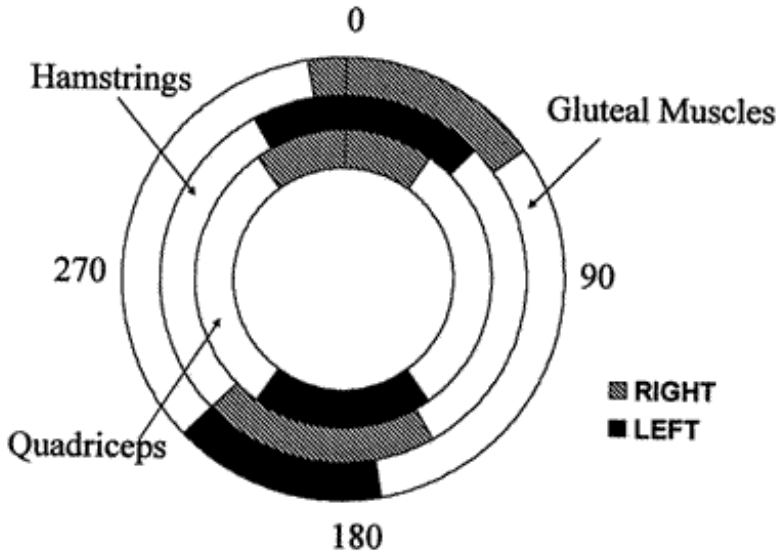

Figure 1.
Pedal cycle and muscle stimulation paradigm schematic. Top dead center for the right crank corresponds to the 0° position in the pedal cycle. Bottom dead center for the right crank corresponds to the 180° position in the pedal cycle. The power phase is defined from 0° to 180°. The recovery phase is defined from 180° to 360°.

Attached to each crank of the bicycle was a custom-built pedal capable of measuring normal (F_N) and tangential (F_T) components of the applied load. Each pedal included a double cantilever design instrumented with standard foil strain gauges (350 Ω) with signals conditioned by a fully active Wheatstone bridge amplifier. The pedals were calibrated prior to the beginning and after completion of the project. Both pedals were linear in each direction (F_N and F_T) ($r^2 = 0.99$) through the range of applied loads (18).

A high-speed cine camera (Photosonics 1-P) operating at a nominal speed of 50 frames per second was used during data collection. The optical axis of the lens was positioned orthogonal to the plane of motion and the film plane was approximately 4 meters from the plane of movement.

Data Acquisition

Data were collected during normal exercise sessions over a 3-month period as each subject enrolled in the FES program (Subject C, then Subject B, and finally, Subject A, in order of collection). Limb displacements (50 frames per second) and pedal force data (200 Hz) were sampled during three successive 10-second trials during each subject's exercise bout. Subject A had difficulty maintaining a minimum crank velocity of 35 RPM, so bicycling was halted three times over a period of 15 minutes. To obtain the desired amount of data, a single trial was collected during each of three brief cycling intervals (1 minute each in duration). Subject B, who just began the bicycling portion of the program, was permitted to cycle for only 5 minutes. Three consecutive trials were obtained from this short, but continuous, bicycling bout. Subject C completed 30 minutes of continuous FES-induced cycling. Data were collected at 5, 15, and 25 minutes of exercise. Joint markers were placed on the subject's hip (approximating the superior border of the greater trochanter), knee (lateral femoral epicondyle), foot-pedal interface (approximating the ankle), and fifth metatarsal-phalangeal (MP) joint (head of fifth metatarsal) of the lower limb facing the camera (right side only). Markers were also placed on the anterior and posterior portions of the pedal, on the pedal spindle, and on the crank axis for the purpose of measuring pedal and crank angle. Anthropometric measurements (e.g., subject height, weight, and lower limb segment lengths) describing each subject were also made.

Pedal forces were synchronized to the kinematic data by a light-emitting diode (LED) placed in the camera field of view being illuminated simultaneously with a 2 V pulse, which transmitted to the data acquisition system (AXOTAPE 1.2, Axon Instruments, Inc.).

Data Reduction

The lower limb was modeled as a planar, three-segment, rigid body system with an external reaction force located at the pedal

spindle.

The linked segment model with all forces and moments acting on each segment is illustrated in **Figure 2.** M_K and M_A are generalized muscle moments (GMMs) at the knee and ankle, respectively, representing the net effect of all muscles and periarticular structures acting about each joint (20). Equations of motion for the two segments were formulated using conventional Newtonian mechanics (Appendix A).

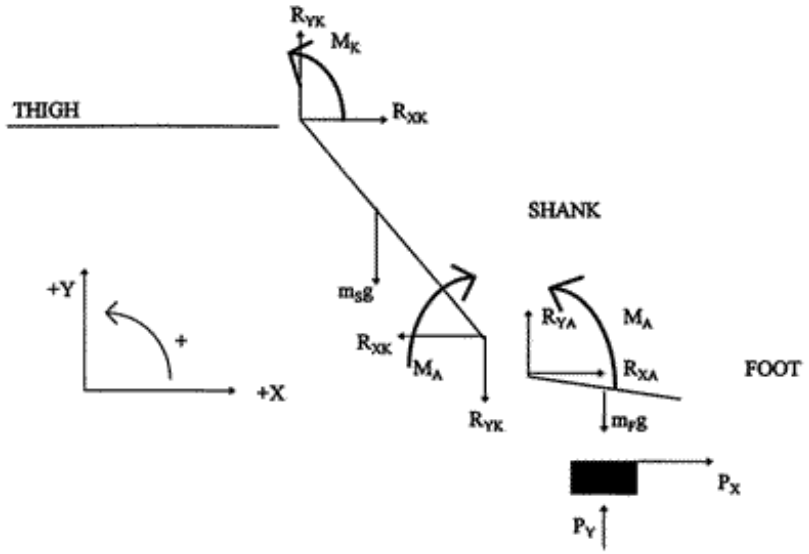

Figure 2.
Free body diagrams for the thigh, shank, and foot segments. Forces and moments acting on each segment are shown. R refers to joint reaction forces in X & Y directions, M refers to generalized muscle moment at the ankle (A) and knee (K), P refers to pedal reaction forces in X & Y directions, mg refers weight of the segment for the shank (S) and foot (F).

Kinematic Data

Coordinate data describing motion of the thigh, shank, foot, pedal, and crank for two revolutions per trial were obtained by digitizing serial film images (Numonics digitizer - IBM XT computer). Time derivatives of linear and angular displacements were computed using finite difference techniques after smoothing algorithms were applied to the original coordinate data.

Smoothing

Cutoff frequencies were determined from a power spectrum analysis, using a technique originally described by Welch (21) and modified by Schneider[1]. A 97 percent cutoff criterion was selected based on visual inspection of the smoothed coordinate data and acceleration (second time derivative) data. Cutoff frequencies were determined individually for each coordinate of each cycle based on the power spectrum analysis. The range of cutoff frequencies varied from 1.5-9.0 Hz for all coordinates across all subjects. Data were smoothed using a fourth order, zero-lag Butterworth filter.

Body Segment Parameters

Anthropometric data (segment mass, center of mass, and moment of inertia) were calculated for each segment using regression equations reported by Winter (22).

Kinetic Data

Normal (F_N) and tangential (F_T) components of the applied pedal force were resolved into global x and y components for inverse dynamics calculations and multiplied by calibration factors to convert volts into Newtons of force.

Equations of Motion

Kinematic data, pedal forces, and body segment parameter data served as input to Newtonian equations of motion designed to calculate joint kinetic profiles. All moments were taken about the center of mass of each segment. Positive forces were assumed to be in the upward direction and positive moments in the counterclockwise direction. In addition to knee-joint reaction forces and moments, effective force delivered to the crank and crank power were calculated. Effective force was the component of the applied force by the foot on the pedal that is aligned perpendicular to the crank. Crank power was defined as effective force * V_{ST} when V_{ST} was the component of the spindle velocity tangential to the crank. Integrating crank power versus cycle time yielded the net work supplied to the right crank during a complete revolution.

Data Analysis

Two revolutions per three trials yielded six revolutions of data per subject. Data from all six revolutions were averaged within a subject.

RESULTS

The results describe the pedaling characteristics of the three subjects. Data were averaged across six pedal resolutions per subject with averages and standard deviations presented in **Table 2** for each subject.

Table 2.

Average (± SD) peak cycling parameters for each subject.*

Parameter	**Subj A**	**Subj B**	**Subj C**
Pedaling rate (RPM)	24±0.4	50±2.0	47±1.0
Maximum extension shank angle (°)	124.8±0.9	133.3±0.2	121.9±0.5
Maximum flexion shank angle (°)	90.9±0.6	97.9±0.4	89.6±0.9
Peak shank extension velocity (°/s)	92.7±9.3	98.1±6.2	85.6±4.8
Peak shank flexion velocity (°/s)	-83.8±0.6	-89.6±3.3	-78.6±2.5
Peak shank acceleration (°/s^2)	619.8±20.5	632.3±86.0	469.6±35.1
Peak positive effective force (N)	191.8±29.7	281.2±22.5	329.0±24.6
Peak negative effective force (N)	-145.3±17.9	-119.5±37.9	-245.6±22.5
Positive crank work (J)	44.9±7.1	48.9±3.4	40.7±6.2
Negative crank work (J)	-76.0±4.2	-25.2±5.8	-55.5±5.6
Peak compressive force (N)	-209.2±51.0	-244.8±19.3	-342.3±6.8
Peak tensile force (N)	90.8±12.9	54.6±4.0	66.5±28.0
Peak posteriorly directed shear reaction force (N)	-34.0±22.0	-114.9±7.2	-159.9±12.9
Peak anteriorly directed shear reaction force (N)	34.6±1.6	29.8±1.2	18.9±11.7
Peak flexor knee moment (N·m)	-13.9±9.5	-51.7±5.0	-72.8±6.1
Peak extensor knee moment (N·m)	12.6±1.1	9.6±1.2	5.3±5.0
Peak knee muscle power absorbtion (W) - power phase	-16.4±6.8	-37.7±5.2	-48.2±9.1
Peak knee muscle power absorbtion (W) - recovery phase	-24.9±1.2	-23.0±10.0	-35.0±7.7

* Average of six trials for each subject; SD = standard deviation; subj = subject.

Timing of critical parameters during the pedal cycle was averaged across the three subjects unless otherwise stated. Exemplar patterns for each subject are presented in **Figures 3-6.**

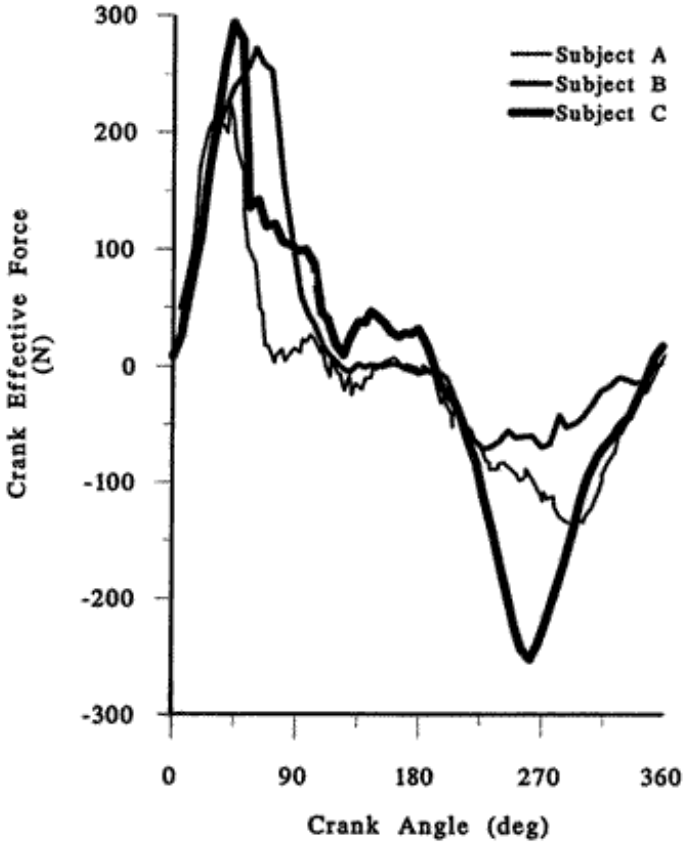

Figure 3.
Average effective force profiles for each subject. Positive values represent a force acting to move the crank in a clockwise direction while negative values represent a force acting to move the crank in a counterclockwise direction.

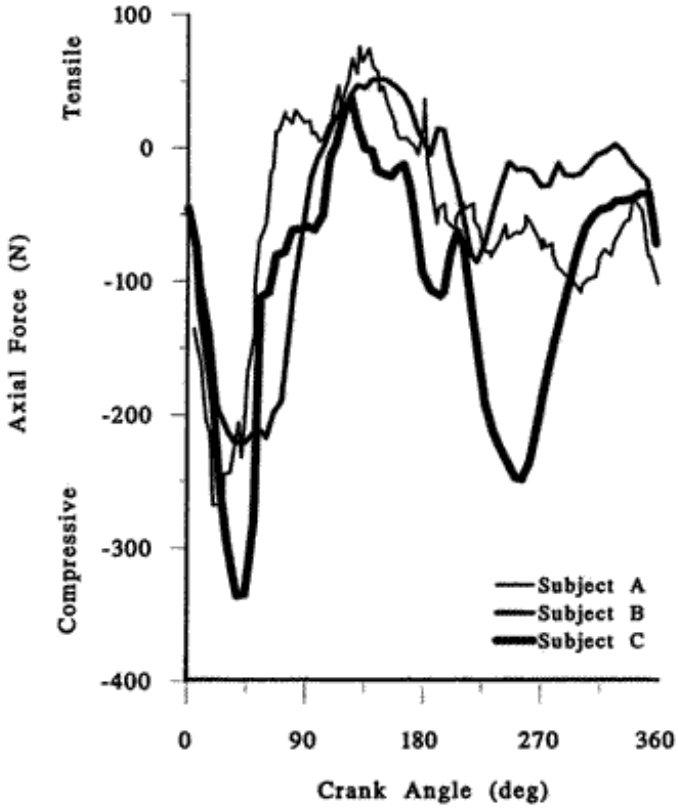

Figure 4.
Average axial reaction force profiles for each subject. Positive values represent tensile loading while negative values represent compressive loading of the knee joint.

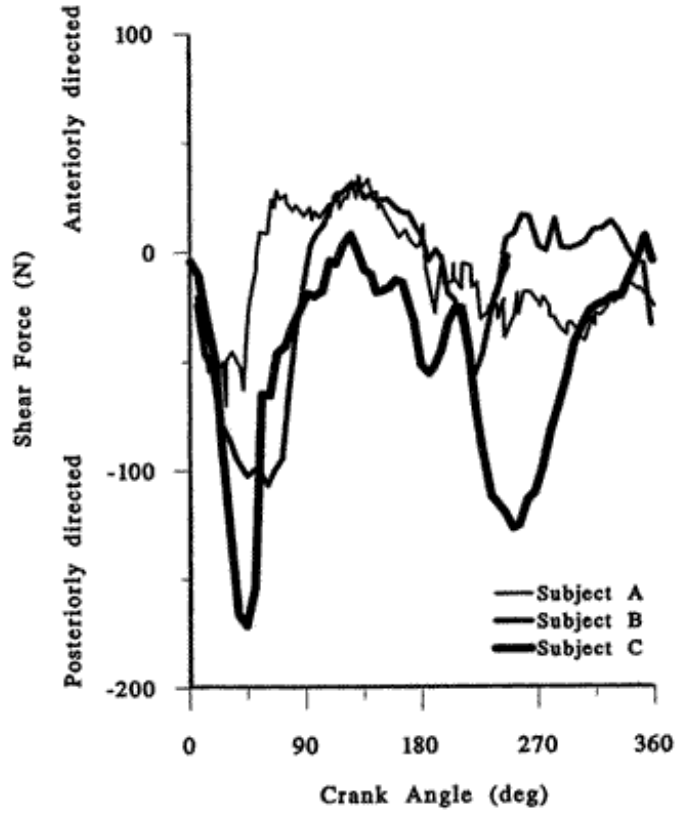

Figure 5.

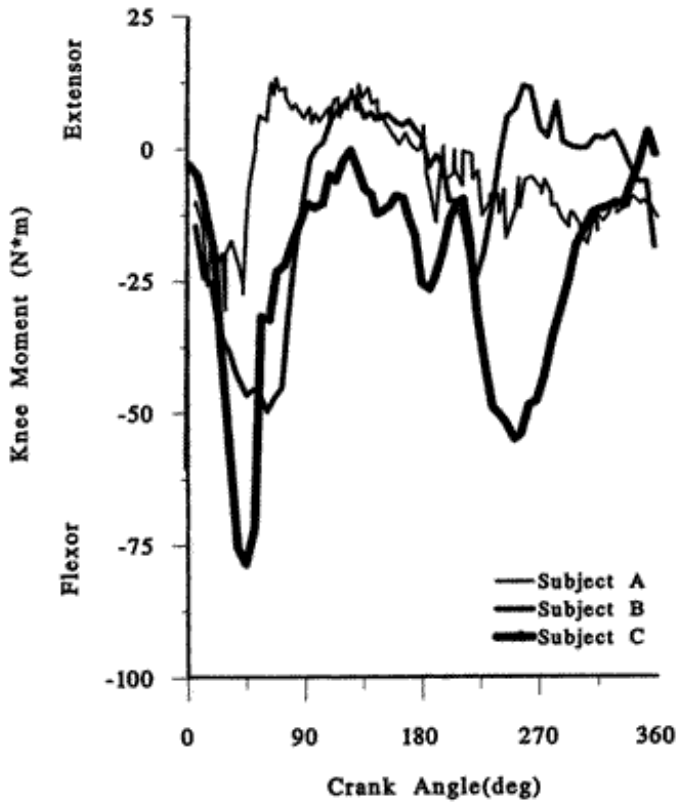

Figure 6.
Average knee generalized muscle moment for each subject.

Average shear reaction force profiles for each subject. Positive values represent forces directed anteriorly along the tibial plateau while negative values represent forces directed posteriorly along the tibial plateau.

Positive values represent extensor moments while negative moments represent flexor moments.

Kinematics

Pedaling rate as calculated from the kinematic data was very consistent within a subject, but Subject A (the most inexperienced with FES) pedaled at a rate half that of the other two subjects. Shank angle patterns displayed a similar shape for all three subjects, although the magnitude was increased at all points throughout the entire pedaling cycle for Subject B. The shank extended through top dead center to maximum extension at 75 ±2° followed by shank flexion until maximum flexion at 249 ±9°. Shank extension occurred during the remainder of the recovery phase. Shank angular velocity was positive during periods of shank extension and negative during periods of shank flexion with a peak flexor velocity occurring just prior to bottom dead center (171 ±4°). Shank angular deceleration occurred during the power phase (0-180°) with the majority of the phase maintaining a steady deceleration rate of 100°/sec^2, followed by rapid acceleration during the recovery phase (180-360°) with the peak at 252 ±3° for Subject B and 272 ±6° for Subjects A and C.

Effective Force and Crank Work

The effective forces generated by Subjects A, B, and C during one revolution, along with muscle stimulation patterns are displayed in **Figure 3.** A positive effective force tended to rotate the right crank in a clockwise direction, while a negative effective force tended to rotate the right crank in a counterclockwise direction. Although differences in magnitude did exist, all three subjects exhibited the following general effective force pattern. Positive effective force occurred during the early portion of the power phase, while the right quadriceps, right gluteal muscles, and left hamstrings were stimulated to extend the right leg. Peak positive effective force magnitude occurred either before or just after the stimulus termination at 54° (Subject A: 38 ±6°; Subject B: 60 ±3°; Subject C: 50 ±5°) followed by a rapid decrease in effective force to near zero during the remainder of the power phase. A negative effective force was observed throughout the recovery phase with a peak at 266 ±15° (Subject A: 292 ±6°; Subject B: 268 ±24°; Subject C: 267 ±3°).

Since subjects pedaled with a relatively constant velocity, crank power showed the same pattern as the effective force. When integrating crank power versus cycle time, crank work was obtained. Only Subject B demonstrated net positive crank work across the entire revolution when adding positive and negative crank work values together.

Knee-joint reaction Forces and Moments

The shank experienced a compressive load when the axial knee-joint reaction force was negative and a tensile load when the axial knee-joint reaction force was positive (**Figure 4**). Positive shear knee-joint reaction forces were directed anteriorly along the tibial plateau, while negative shear knee-joint reaction forces were directed posteriorly along the tibial plateau (**Figure 5**). A positive knee moment represented an extensor knee moment, while a negative knee moment represented a flexor knee moment (**Figure 6**).

Knee-joint reaction force loading patterns were similar across all three subjects, although magnitudes were considerably different. Large compressive forces were experienced at the knee during the first 90° of the power phase as the right gluteal and quadriceps muscles were stimulated (**Figure 4**). Peak compressive forces occurred prior to stimulus termination at 54° (Subject A: 31 ±4°; Subject B: 48 ±13°; Subject C: 46 ±7°). During the remainder of the power phase, a small tensile force was observed with a peak occurring at 136 ±11° (range: 127-149°), just prior to initiation of muscle stimulation. Axial reaction forces were again compressive during the recovery phase. Shear reaction forces followed a similar pattern to the axial reaction forces. Negative (posteriorly directed) reaction forces during the initial 90° of the power phase were followed by small positive (anteriorly direction) reaction forces during the remainder of the power phase (**Figure 5**).

Knee muscle moments (**Figure 6**) also followed a similar pattern to the joint reaction forces. A large peak flexor moment occurred before or just following the stimulus termination (Subject A: 35 ±6°; Subject B: 63 ±6°; Subject C: 54 ±13°) during the time of shank deceleration, but prior to maximum shank extension angle. Subject A demonstrated a transition to extensor knee moment prior to the other subjects and this subject's peak extensor knee moment was larger and earlier in the pedal cycle (Subject A: 69 ±5°; Subject B: 156 ±39°; Subject C: 111 ±37°). Knee moments during the recovery phase were variable as transitions to flexor and back to extensor were observed in Subjects A and B but consistently flexor in Subject C. Since knee muscle moments were generally opposite in direction to shank movement during the power phase, knee muscle power was absorbed.

DISCUSSION

This preliminary study described the knee-joint reaction forces and pedal effectiveness parameters generated by three subjects with chronic SCI during FES-induced bicycling. There were three critical findings: 1) pedaling effectiveness was severely compromised in

this subject population as indicated by a lack of overall positive crank work, 2) knee-joint kinetics were similar in magnitude to data reported for unimpaired individuals pedaling at higher rates and workloads suggesting excessive knee-joint loading for subjects with SCI, and 3) shear reaction forces and muscle moments were opposite in direction to data reported for unimpaired individuals revealing an energetically unfavorable knee stabilizing mechanism.

While remarkable similarities were apparent between data reported for unimpaired bicyclists riding the upright bicycle and the contralateral lower limbs (limb opposite the involved lower limb and ipsilateral to the lesion) of subjects with CVAs riding a recumbent bicycle, especially during the power phase (18), knee-joint kinetics observed in the SCI subjects riding the ergometry system were substantially different from data reported for unimpaired bicyclists riding the upright bicycle. Differences in recovery phase patterns exhibited by the contralateral lower limbs of subject with CVAs on a recumbent bicycle and patterns reported for unimpaired bicyclists on an upright bicycle most likely resulted from limitations of the involved lower limb in generating power during its power phase--recovery phase of the contralateral lower limb (18). Differences in knee-joint kinetics between data reported for unimpaired bicyclists and SCI subjects on the ergometry system, however, were most likely due to muscle stimulation paradigm differences with actual muscle activity data (17) and bicycle configuration.

Effective force patterns presented by Cavanagh and Sanderson (16) were positive during the power phase and negative during the recovery phase. Data from this investigation showed similar patterns for the subjects with SCI, although the percentage of the pedal cycle in which positive effective force occurred was reduced. While peak positive effective force magnitude was expected to be reduced in subjects with SCI relative to unimpaired subjects due to the reduction in pedaling rate and workload, peak negative effective force was increased in the subjects with SCI relative to the unimpaired subjects.

Compressive axial reaction forces were similar in magnitude during the power phase to those reported for unimpaired bicyclists pedaling at rates that were almost double (90 RPM) and a substantially higher workload--225W (15). Additionally, large compressive axial reaction forces occurred during the recovery phase of SCI bicyclists, but have not been reported for unimpaired bicyclists (15,17). The increase in knee loading in SCI subjects may cause concern regarding fracture risk. Studies on bone compressive strength suggest that a reduction in bone density to one-third of normal values is common in persons with spinal cord injury and may result in a bone compressive strength reduction to one-ninth of normal values (23). This has important consequences to SCI subjects as bone loss reaches fracture threshold at the knee (1 gm/cm^2) within 16-months post SCI (24). Thus, FES-induced bicycling may generate compressive forces large enough to produce a fracture in the weakened lower limbs of individuals with SCI.

Posteriorly directed shear reaction forces produced by subjects with SCI were opposite in direction relative to those reported for unimpaired bicyclists (15,17). The reversal in shear reaction-force direction at the knee appears to be the result of differences in bicycle configuration. Upright bicycling geometry positioned the rider nearly on top of the crank origin, placing the shank posterior to the knee throughout much of the power phase. As a result, forces transmitted from the femur to the tibia were directed both axially and *anteriorly* along the tibial plateau. During FES-induced bicycling, the rider sat from 1 to 3 feet behind the crank origin. This unique configuration positioned the shank anterior to the knee throughout the entire power phase. Force transmitted from the femur to the tibia was directed axially and *posteriorly* along the tibial plateau.

The direction in which shear reaction force acts at the knee has a significant effect on joint stability. Anteriorly directed shear reaction force generated by unimpaired bicyclists would tend to destabilize the knee anteriorly. The burden to prevent anterior displacement of the tibia relative to the femur would be placed upon anterior knee structures: the quadriceps tendon, patella, and anterior cruciate ligament. Additionally, the knee extensor muscle moment observed during the power phase (25) reflects contraction of the quadriceps to force the patella into the femur to prevent the anteriorly directed shear reaction force from disarticulating the knee. Posteriorly directed shear reaction forces exerted by the femur on the tibia during FES-induced bicycling would tend to destabilize the knee posteriorly. Structures deterring posterior translation of the tibia relative to the femur may include the hamstring muscles and posterior joint capsule. While the hamstring musculature does not receive stimulation until almost the completion of the power phase, the observed knee flexor muscle moment during FES-induced bicycling may result from the development of passive tension from the posterior knee-joint structures to prevent posterior disarticulation of the knee joint.

The last critical finding of this study was that pedaling effectiveness was severely compromised in this subject population. While unimpaired bicyclists generate power during the power phase as a result of the knee extensor moment acting during knee extension (25), subjects with SCI absorb power during the power phase of FES-induced bicycling due to the knee flexor muscle moment occurring during knee extension. Power absorption sustained during the power phase of FES-induced bicycling increases muscle workload and may decrease mechanical efficiency. Thus, bicycle configuration may play a role in producing mechanical efficiency and joint stabilization. In the upright bicycle configuration used by unimpaired bicyclists, thigh and leg orientation place the shank behind the knee throughout the power phase permitting energy-efficient knee stabilization to occur, resulting in an anteriorly directed shear reaction force and enabling the quadriceps to efficiently stabilize the knee joint. Additionally, changes in seat height to increase knee flexion, which effectively places the shank further posterior to the knee, increase anteriorly directed shear reaction forces (17). This has implications for the use of the bicycle in rehabilitation, since reduced seat heights reduce anterior tibial strain in persons with anterior cruciate ligament-deficiency (17). Such modification to the FES cycling configuration may also reduce stress on the passive knee structures and increase cycling duration, yielding improved aerobic benefit.

The fact that power was absorbed at the knee during the power phase of FES-induced bicycling raises the question as to how movement is produced. Numerous studies have reported that the gluteal muscles, through active extension of the thigh, may play a major role in producing the motion achieved by unimpaired bicyclists (25-27). Although thigh kinematics and hip moments were not calculated in this study, effective force and muscle stimulation plots suggest that the gluteal muscles play a similar role during FES-induced bicycling. The muscle activation paradigm utilized by the microprocessor (**Figure 1**) terminates the quadriceps stimulation at 35° and gluteal muscle stimulation at 54°. Peak positive effective force magnitude occurred either before or just after the stimulus termination at 54° followed by a rapid decrease in effective force to near zero during the remainder of the power phase. Continued force production throughout the interval between quadriceps and gluteal muscle stimulation termination implies that the gluteal muscles are the primary source of power for FES-induced bicycling. Further research involving hip moments is needed to accurately assess gluteal muscle function during FES-induced bicycling.

CONCLUSION

Knee-joint kinetic analysis has yielded useful insight into the FES-induced bicycling task. Knee-joint reaction forces and pedal forces have been shown to be substantial and strikingly similar in magnitude to loads generated by unimpaired bicyclists: in some cases, even exceeding forces produced by unimpaired bicyclists. Such force magnitudes, although moderate in comparison to loads generated during activities such as running, may be large enough to produce a fracture in the compromised lower limbs of the individual participating in FES-induced bicycling. Further study focusing on the actual bone stresses produced during FES-induced bicycling is required to accurately assess the presence of any potential fracture risk. In addition, knee-joint moments have been measured and analyzed in conjunction with leg kinematics profiles to reveal an energetically unfavorable knee stabilizing mechanism.

The results of this study, although significant, provide only an initial view into FES-induced bicycling mechanics. Further research involving geometry alterations and load dynamics must be conducted if future FES-induced cycling systems are to maximize both the cardiopulmonary and musculoskeletal benefits associated with this unique form of therapy.

REFERENCES

1. BeDell KK, Scremin AME, Perell KL, Kunkel CF. Effects of functional electrical stimulation-induced lower extremity cycling on bone density of spinal cord injured patients. Am J Phys Med 1996;75:29-34.
2. Kiralti BJ, Sims G, Perkash I. Fracture occurrence and healing in the spinal cord injured population. Proceedings of the 40th Annual Conference of the American Paralysis Society; 1994.
3. LeBlanc A, Schneider VS, Evans HJ, Engelbretson DA, Kreb JM. Bone mineral loss and recovery after 17 weeks of bed rest. J Bone Mineral Res 1990;5:843-50.
4. Whedon GD. Disuse osteoporosis: physiological aspects. Calcified Tissue Inter 1984;36:S146-50.
5. Tipton CM. Considerations for exercise prescriptions in future space flights. MSSE 1983;15:441-4.
6. Stout SD. The effects of long-term immobilization on the histomorphology of human cortical bone. Calcified Tissue Inter 1982;34:337-42.
7. Minaire P. Immobilization osteoporosis: a review. Clin Rhuematol 1989;8:95-103.
8. Buford JA, Zernicke RF, Smith JL. Adaptive control for backward quadrupedal walking I. Posture and hindlimb kinematics. J Neurophysiol 1990; 64:745-55.
9. Shaw S, Zernicke RF, Vailas AC, Dluna D, Thomason D, Baldwin K. Mechanical, morphological and biochemical adaptations of bone and muscle to hindlimb suspension and exercise. J Biomech 1987; 20:225-34.
10. Hangartner TN, Rodgers MM, Glaser RM, Barre PS. Tibial bone density loss in spinal cord injured patients: effects of FES exercise. J Rehabil Res Dev 1994;31:50-61.
11. Leeds EM, Klose KJ, Ganz W, Serafini A, Green BA. Bone mineral density after bicycle ergometry training. Arch Phys Med Rehabil 1990;71:207-9.
12. Pacy PJ, Hesp R, Halliday DA, Katz D, Cameron G, Reeve J. Muscle and bone in paraplegic patients and the effect of functional electrical stimulation. Clin Sci 1988;75:481-7.
13. Rodgers MM, Glaser RM, Figoni SF, et al. Musculoskeletal responses of spinal cord injured individuals to functional neuromuscular stimulation-induced knee extension exercise training. J Rehabil Res Dev 1991;28(4):19-26.
14. Kunkel CF, Scremin AME, Eisenberg B, Garcia J, Roberts S, Martinez S. Effect of "standing" on spasticity, contracture, and osteoporosis in paralyzed males. Arch Phys Med Rehabil 1993;74:73-8.
15. Ruby P, Hull ML, Hawkins D. Three-dimensional knee joint loading during seated cycling. J Biomech 1992;25:41-53.
16. Cavanagh PR, Sanderson DJ. The biomechanics of cycling: studies of the pedaling mechanics of elite pursuit riders. In: Burke RE, editor. Science of cycling. Champaign, IL: Human Kinetics Books; 1986. p. 91-122.

17. Gregor RJ, Fowler EG. Biomechanics of cycling. In: Zachazewki J, Magee D, Quillen W, editors. Athletic injuries and rehabilitation; 1996. p. 367-88.
18. Perell KL, Gregor RJ, Scremin AME. Lower limb cycling mechanics in subjects with unilateral cerebrovascular accidents. J Appl Biomech 1998;14:158-79.
19. Ragnarsson KT, Pollack S, O'Daniel W, Edgar R, Petrofsky J, Nash MS. Clinical evaluation of computerized functional electrical stimulation after spinal cord injury: a multicenter pilot study. Arch Phys Med Rehabil 1988;69:672-7.
20. Hoy MG, Zernicke RF, Smith JL. Contrasting roles of inertial and muscle moments at knee and ankle during paw-shake response. J Neurophysiol 1985;54:1282-98.
21. Welch PD. Modified periodogram method for power spectrum estimation. IEEE Trans Audio Elect 1967;15:70-3.
22. Winter DA. Biomechanics and motor control of human movement. New York: John Wiley & Sons; 1990.
23. Carter DR, Hayes WC. Bone compressive strength: the influence of density and strain rate. Science 1976;194:1174-6.
24. Garland DE, Stewart CA, Adkins RH, et al. Osteoporosis after spinal cord injury. J Orthop Res 1992;10:371-8.
25. Gregor RJ, Cavanagh PR, LaFortune M. Knee flexor moments during propulsion in cycling: a creative solution to Lombard's paradox. J Biomech 1985;18:307-16.
26. Gregor RJ, Broker JP, Ryan MM. The biomechanics of cycling. ESSR 1991;127-69.
27. Ryan MM, Gregor RJ. EMG profiles of lower extremity muscles during cycling at constant workload and cadence. J Electromyogr Kinesiol 1992;2:69-80.

Contents

Back to Top